Objective Analysis of Discontinuous Satellite-Derived Data Fields for Grid Point Interpolation

ALAN E. LIPTON AND DONALD W. HILLGER

Department of Atmospheric Science, Colorado State University, Fort Collins, CO 80523

31 March 1982 and 11 July 1982

ABSTRACT

In retrieval of atmospheric temperature and moisture soundings from satellite infrared radiance measurements the raw data commonly used consist of dense fields of radiances interrupted by data-free gaps. This note reports an objective analysis procedure which was developed to specifically handle data fields of a discontinuous nature. The method is a correlation-weighted interpolation scheme and includes an oval-extension gap filling feature. Test cases demonstrate the ability of the program to fill gaps caused by instrument calibration periods and by data contamination due to clouds. The procedure is shown to produce much better results within a data-free region than does a similar method without the gap filling feature. An application of this method is also shown in a comparison of satellite-derived atmospheric parameters with conventional observations on a point-to-point basis. However, applications of the procedure are not limited to satellite data analysis, but could include analyses of aircraft data and data from ocean buoys.

1. Introduction

Much attention is currently being devoted to the production of accurate atmospheric soundings of temperature and moisture using high-resolution satellite-based radiometers. The primary source of information on which such soundings are based is a field of radiances measured by a satellite. However, a frequently encountered problem occurs when these radiance fields are interrupted by data-free gaps resulting from calibration periods of the measuring instrument, erroneous data, or contamination of the data by clouds. This problem can be alleviated provided that data can be interpolated into the gaps from surrounding areas, thus producing a complete field of atmospheric parameters.

The purpose of this research was to develop an objective analysis procedure tailored specifically to handle dense data fields which contain data-free areas. Analysis of such fields involves a unique problem because of the discontinuity of data density. In order to retain the high resolution of the original data set the interpolation scheme should do a minimum of smoothing in areas of high data density. However, in data sparse areas the scheme should produce a relatively smooth interpolation since no fine detail is known within these regions. In addition to the filling of gaps in data, the analysis procedure was expected to produce an output format that can be easily used in both research and forecasting as a tool for assessing the characteristics of fields of either radiances or temperature and moisture retrievals.

The type of objective analysis dealt with in this paper is of the spatial variety. Methods of this sort are used when the object is to construct a two-dimensional field of data at a single measurement time. For example, the purpose might be to initialize a numerical model using data from one satellite pass. Should the object instead be to incorporate observations taken at different times then the problem becomes one of temporal interpolation or time-continuous data assimilation. These latter subjects are dealt with elsewhere (e.g., Ghil *et al.*, 1979).

One commonly used method of spatial analysis is an iterative technique proposed by Barnes (1964). That approach proved to be inappropriate for data fields of greatly varying density. The analysis method finally chosen for this study is not based on a rigorous derivation but is instead an adaptation of previously derived methods. Basically, the scheme consists of a non-iterative version of the Barnes technique with a number of modifications. An important change was inspired by the works of Gandin (1963) and Thiebaux (1975) which suggest that the autocorrelation function of a data field will provide a useful weighting scheme for the interpolation to grid points.

2. Test cases

The data sets which were analyzed consist of temperature, water vapor and window channel radiances from the TIROS Operational Vertical Sounder (TOVS). The radiances were measured over the central United States on 30 September 1980 by the TIROS-N and NOAA-6 polar orbiting satellites at ap-

0021-8952/82/101571-11$06.75

proximately 1000 and 1400 GMT, respectively. Calibration gaps occur in both data sets.

In addition to the calibrated TOVS radiance measurements this analysis method was also applied to retrieved values of precipitable water, stability parameters and dew point temperatures which were derived at various levels from those radiances. The retrieval method for these various meteorological parameters was similar to that described by Hillger and Vonder Haar (1981). The processed data were used in an attempt to test the capability of the method to interpolate a complete field of satellite-derived meteorological parameters. This type of data can be used more directly than simple radiances in meteorological analysis and forecasting.

3. The analysis

a. Filtering

The first step in objectively analyzing a data set is the filtering out of input data points which are obviously erroneous. This is done by comparing each data value to the average value of the three nearest points. A point is eliminated if the examined value deviates from the surrounding mean by more than two times the standard deviation of the whole data set. In other terms, if

$$\left| V_0 - \frac{V_1 + V_2 + V_3}{3} \right| \geq 2\sigma, \qquad (1)$$

where V_i is a data value and σ the standard deviation, then point V_0 is eliminated. The multiplier value of 2 was empirically chosen from several test cases in which it successfully differentiated between strong gradients and bad data, thus allowing strong but not extreme gradients to be retained.

A filtering procedure of this kind succeeds only in eliminating isolated groups of one to three points which deviate strongly from the surrounding data. Larger clusters of bad data may be eliminated either manually or automatically during the temperature-moisture retrieval process.

b. Interpolation

The objective analysis scheme which was applied to the filtered data works basically as follows, with the purpose being to fill a regular grid over some geographical area with interpolated values of an atmospheric parameter. Each grid point is considered individually, with the value assigned at that point determined by a weighted average of all those given data points which lie within some specified distance of the grid point. That distance was termed the "radius of consideration" (ROC) (see Fig. 4). Therefore, if there are to be a total of N interpolation grid points, then the values of the interpolated meteorological parameters P_k are given by

$$P_k = \frac{\sum_{j=1}^{M} W_{jk} P_j}{\sum_{j=1}^{M} W_{jk}}; \quad k = 1, 2, \ldots, N, \qquad (2)$$

where M is the number of given data values P_j within the ROC about grid point k, and W_{jk} are the weighting factors. The denominator in (2) is a normalization factor.

c. Weighting factors

The weighting factors assigned to considered data values are a decreasing function of distance between the data point and the grid point, with that function being determined through statistical analysis of the data field. This is done by examining all possible pairs of input data points in order to compute the autocorrelation as a function of pair separation distance only.[1] The isotropic correlations are computed in the form of averages over specified range gates (Hillger and Vonder Haar, 1979). For example, a correlation of 0.83 may be computed for points separated by 50 ± 12.5 km. A least-squares best-fit curve is then applied to these discrete values thereby providing a continuous curve which is used as the weighting function (Fig. 1). In choosing a functional form for the fitting procedure the work of Thiebaux (1975) was considered, although we did not face the constraints encountered in that study of geostrophic geopotential surface analysis. We were therefore able to use a simple decreasing exponential of the form

$$\text{Corr}(x) = \exp(-ax^2), \quad \text{where} \quad x = \text{distance}, \qquad (3)$$

which proved accurate and expedient in the fitting procedure.[2] The weighting factors may then be derived from the coefficient determined in (3) by using

$$W_{jk} = \exp(-aS_{jk}^2), \qquad (4)$$

where S_{jk} is the distance between data point j and grid point k.

d. Standard analysis

Given a method for computing the weighted averages it is necessary to apply it in a manner that achieves the previously mentioned goal of showing field detail which is appropriate to data density. A simple approach is to employ a radius of consideration which expands incrementally until it is just large

[1] For this study no consideration was given to directional orientation of pairs of measurements in computing autocorrelations.

[2] The use of a function of this kind assumes that the autocorrelation equals unity at zero separation distance (i.e., no error in the data). Although there in fact is some error present, this assumption seems to have made a minimal impact on the shape of the fitted curve.

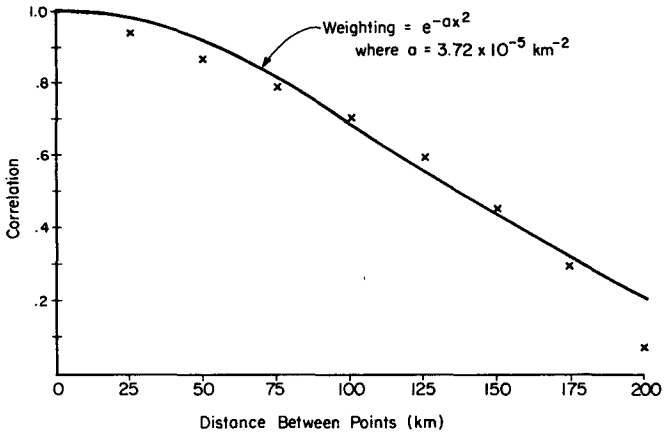

FIG. 1. Correlation plotted as a function of distance as computed from the data shown in Fig. 2b. The plotted values are averages over 25 km range gates. The weighting function is a least-squares best-fit curve applied to the correlation values shown here.

enough to encompass four data points (Thiebaux, 1975), so that $M = 4$ in Eq. (2). This method proved to be skillful at reproducing the features of data-dense regions, but it failed to interpolate well into data-void gaps.

The qualities of the basic analysis are illustrated by Figs. 2a–2c. Fig. 2a shows a complete field of radiances at 7.32 μm, which is a water vapor channel with the peak emission source near 70 kPa. The GOES-E visible image taken about one-half hour later shows that the area was mostly cloud free (Fig. 3). A strip of data was removed from the radiance field to provide a test case for gap-filling skill (Fig. 2b). The above described analysis is shown in Fig. 2c where it can be seen that the contours have been bunched about the center of the gap. The bunching occurs because interpolation to grid points just above gap center was based entirely on weighted data points from the top edge of the gap, whereas grid points just below gap center were filled using data from the bottom edge only. Gap edge features are therefore stretched to the center of the gap and the gradient is concentrated there. If such an analysis were used as input to a numerical model the results could be highly distorted.

It is necessary at this point to make a few additional comments about this objective analysis method. Recall that each grid value P_k is computed as a weighted average of actual data P_j rather than using deviations of P_j from values that had been forecast for the current analysis time, and that the computation of P_k includes a normalization factor. These considerations imply that all grid value computations are based entirely on the current data set, and there is no tendency for interpolation within data-sparse areas to neglect the current data source because of low absolute weights. Analysis schemes which rely on adjusting a forecast to reflect the most recent data could potentially produce a poorly analyzed field when data density varies greatly. If the current measurements are meteorologically inconsistent with a poor forecast (a real possibility in data-sparse regions), then artificial fluctuations might be produced in the area of a gap such as that depicted in Fig. 2b. A method which uses only the current data would not encounter that problem. The trade-off, of course, is that with this method any available observations taken before the current analysis time are neglected.

e. Oval-extension analysis technique

An effort was made to provide improved gap filling capability by modifying the above scheme in the following manner. As the ROC is expanded about a grid point in search of four data points, it is noted whether the ROC becomes greater than a gap indicating limit. Here that limit was chosen to be $2d$, where d is the distance between the pair of given data points which are closer to each other than any other pair.

Once it has been determined that the considered grid point lies in a gap, that point is handled in two special ways. First, the ROC will not stop expanding until it includes five or more data points, rather than the original four. This provides a greater degree of smoothing. Second, once at least two points have been found, it is determined whether they are all found within any one-third of the field relative to the grid point (see Fig. 4). If so, the ROC is not isotropically expanded to find more points as the dashed circle R_2 in Fig. 4 would indicate. Instead, the ROC becomes eccentric to search further in the opposing direction to the previously found data. This new ROC is the solid line labeled R'_2 in Fig. 4, and is given by

$$R'_i(\alpha) = R_i + \tfrac{2}{3}\Delta Rn \cos\alpha, \qquad (5)$$

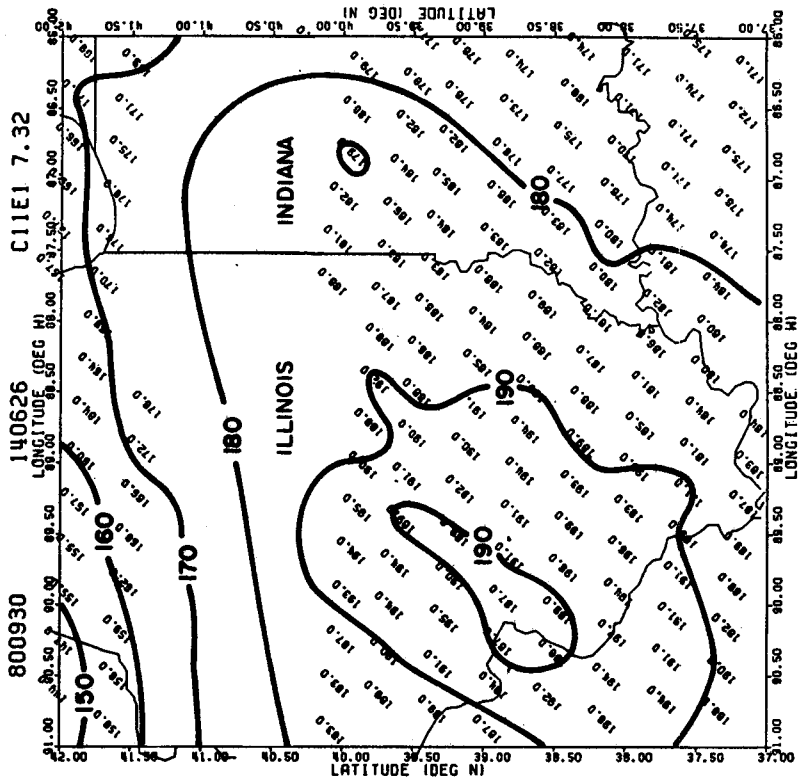

FIG. 2b. As in Fig. 2a with some data removed to simulate a calibration gap.

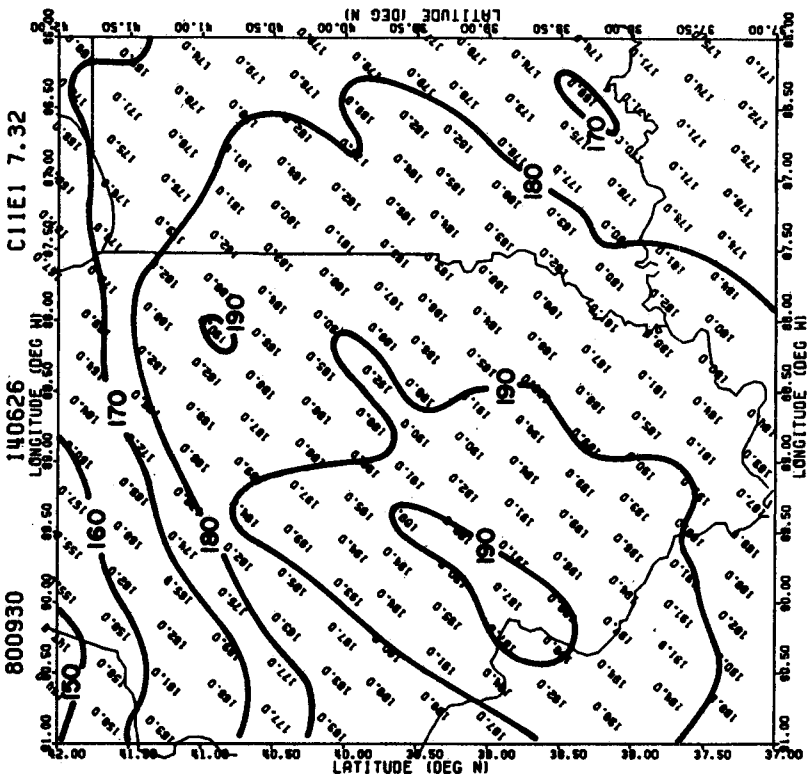

FIG. 2a. Data field of 7.32 μm radiances as measured by TOVS on 30 September 1980 at about 1400 GMT over Illinois and Indiana. The radiances are in units of 10^{-1} mW m^{-2} sr^{-1} (cm^{-1})$^{-1}$ with hand-drawn contours every ten units.

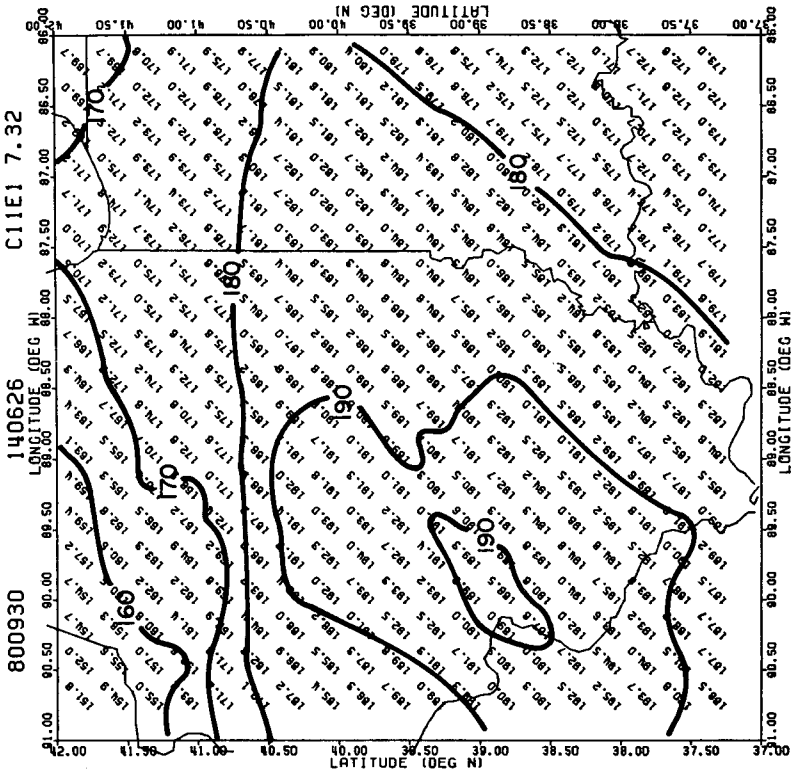

FIG. 2d. Objective analysis of the field in Fig. 2b including the oval-extension gap filling feature. The hand-drawn contours demonstrate the difference in gradient at about 40.5° latitude as produced by this analysis and that in Fig. 2c.

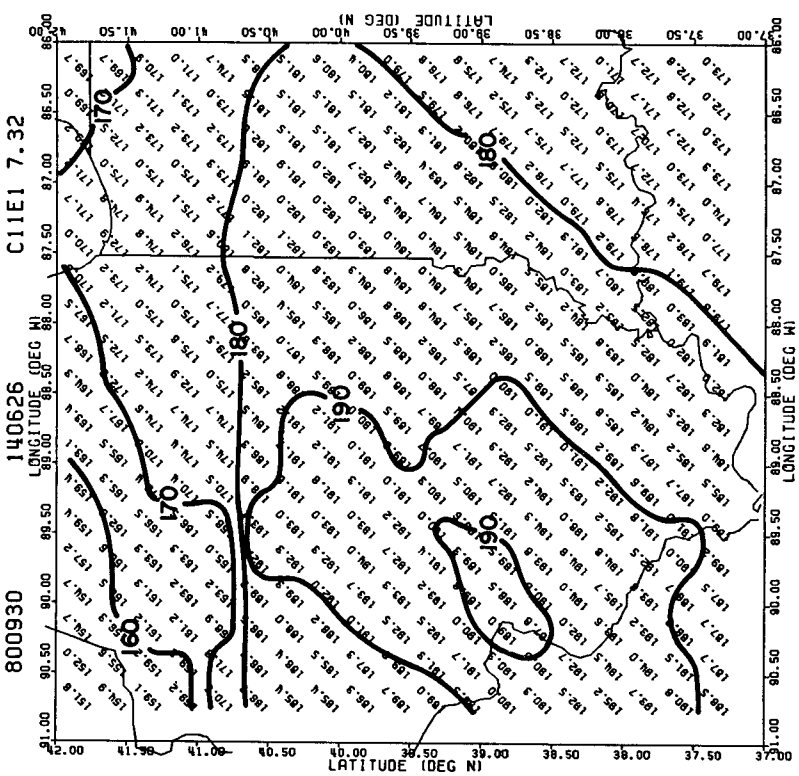

FIG. 2c. The standard analysis of the field in Fig. 2b with hand-drawn contours.

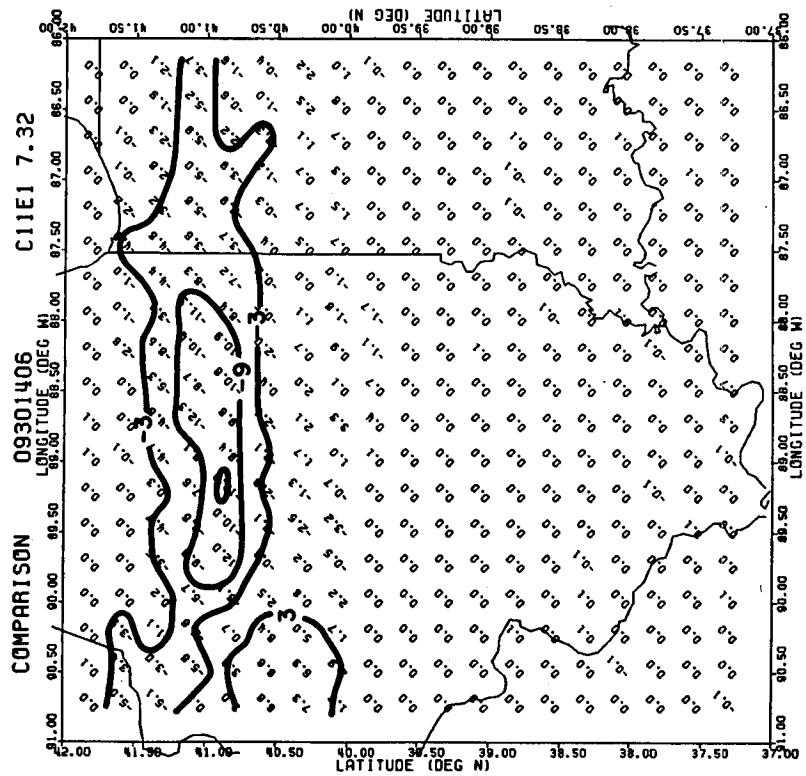

FIG. 2f. As in Fig. 2e except that the differences were calculated using the data of Fig. 2d instead of 2c. This shows a slight improvement in absolute error over that in Fig. 2e. That improvement is due to the gap-filling feature included in the Fig. 2d analysis.

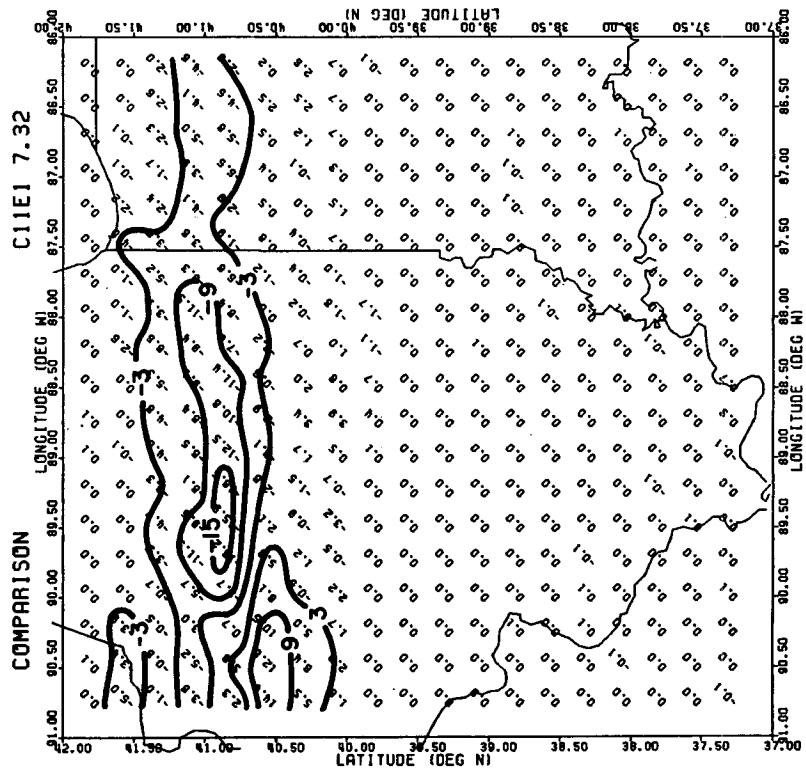

FIG. 2e. A hand-contoured plot of the difference between the analyzed field in Fig. 2c and a standard analysis of the original field of Fig. 2a (the latter analyzed field is not shown). The numbers plotted here are a measure of the error the standard analysis suffered as a result of the removal of a strip of data. Contours are every 0.6 mW m^{-2} sr^{-2} $(cm^{-1})^{-1}$.

where $R'_i(\alpha)$ is the eccentric ROC, ΔR the expansion increment of the ROC = $d/20$, R_i the circular ROC = $R_0 + i\Delta R$, i the number of ROC expansions about this grid point, n the number of ROC expansions since eccentricity was implemented, and α the angular deflection from the extension axis. The object is to fill central parts of the gap with contributions of information from both edges.

The result of implementing the gap-filling feature can be seen in Fig. 2d where it is clear that the change has produced a much more realistic interpolation within the gap region than did the standard analysis. While examination of Figs. 2a–2d serves as a useful method to assess the gradient reproduction capabilities of the analysis methods, another comparison method is also useful. In Figs. 2e and 2f the fields in Figs. 2c and 2d, respectively, are compared to a simple analysis of the field in Fig. 2a, which serves as a control. The "errors" which are plotted there show a slight improvement in an absolute sense by using the oval-extension feature.

The analysis methods may also be compared in an objective manner through examination of the plots shown in Figs. 5a and 5b, which denote the radius of consideration and the number of data points considered at each grid point corresponding to analyses 2c and 2d, respectively. The thoroughness with which plots of this kind describe the qualities of the analysis makes them valuable tools for a user of this objective analysis procedure. The contours shown in Fig. 5 delineate areas of low data density thus elucidating the fact that the user should place less confidence in interpolated values within those regions.

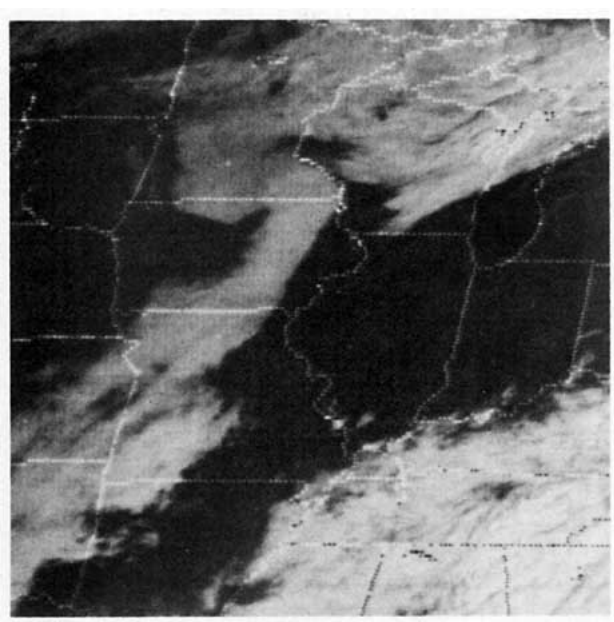

FIG. 3. The GOES-E visible image taken at 1430 GMT on 30 September 1980. Note the band of fog extending through central Iowa and the clear area over Illinois and Indiana.

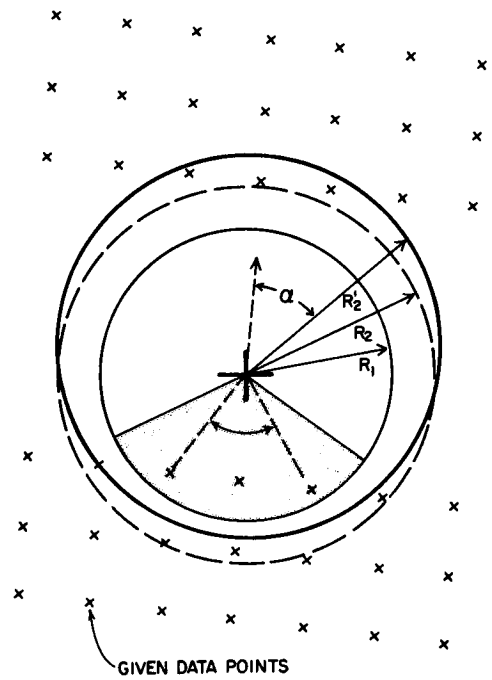

FIG. 4. A schematic depiction of the oval-extension analysis feature. The large cross in the middle represents an interpolation grid point which lies within a data-free gap. R_1 is the circular radius of consideration (ROC) which first encounters at least two grid points. The dashed lines indicate the directionality associated with the points whose angular separation lies within the shaded boundary. R_2 indicates a uniformly expanded ROC while R'_2 denotes an ovally expanded ROC according to Eq. (3).

f. Applications of the method

In order to further test the capabilities of the oval-extension objective analysis procedure it was applied to a case of cloud-contaminated satellite measurements. Fig. 6a shows a field of retrieved values of dew point temperature at the 70 kPa level at 1400 GMT with a large number of values unobtainable due to the presence of clouds.[3] The GOES-E visible image at 1430 GMT shown in Fig. 3 covers this area and shows the cloudy region where satellite-based retrievals were not available. The analysis of this region (Fig. 6b) demonstrates that the procedure utilized here can provide a reasonable interpolation even for very large data gaps. It should be noted, however, that the analysis failed to accurately reproduce the strong gradient in eastern Iowa because that gradient occurred along the gap edge and with little supporting data.

Another example of the usefulness of an analysis procedure such as the one described in this note is shown in Fig. 7. Synoptic surface observations of dew point temperature at 1200 and 1500 GMT were ob-

[3] Cloudiness was determined for each point by examining the brightness temperature difference between window channels at 3.7 and 11.0 μm (Dozier, 1980).

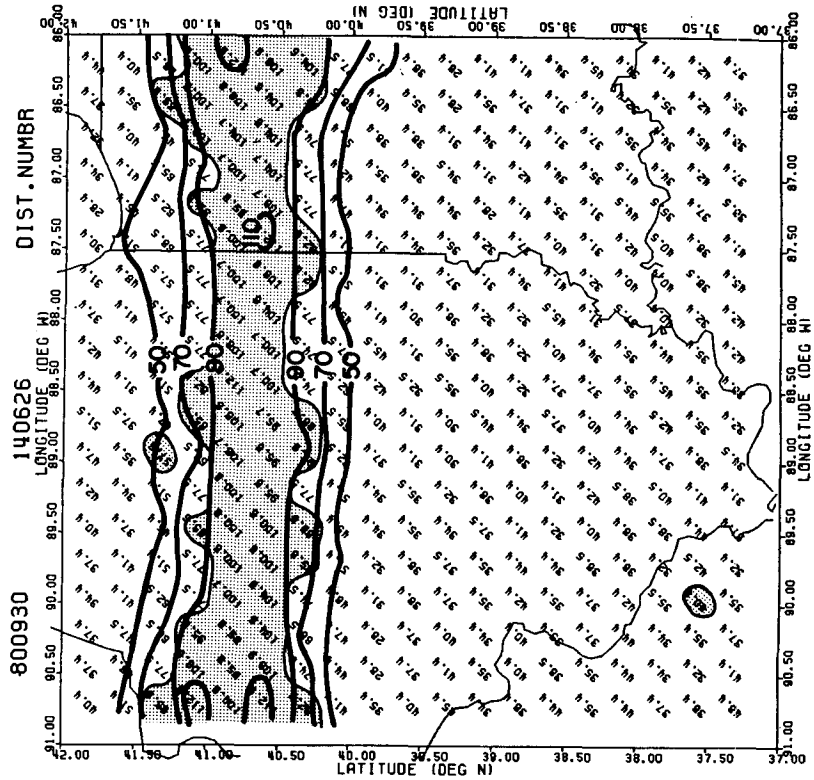

FIG. 5b. As in Fig. 5a except that this plot corresponds to Fig. 2d.

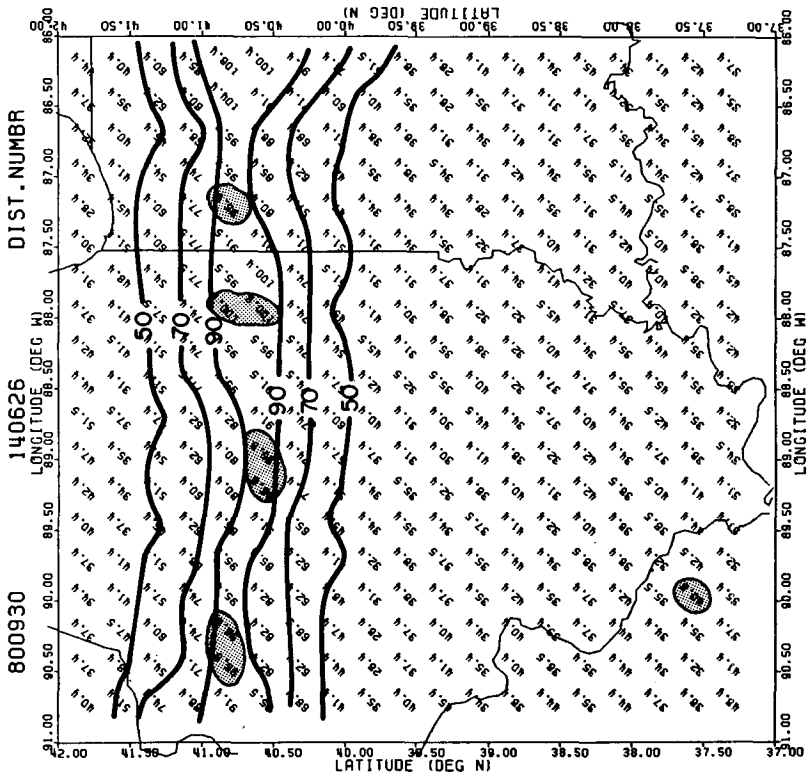

FIG. 5a. A plot of radius of consideration and number of data points considered at each grid point for the analysis shown in Fig. 2c. The radius (km) is given before the decimal point and is contoured at 20 km intervals starting with 50 km. The data point counter follows the decimal and is shaded for values greater than 6. Shading indicates increased smoothing during interpolation.

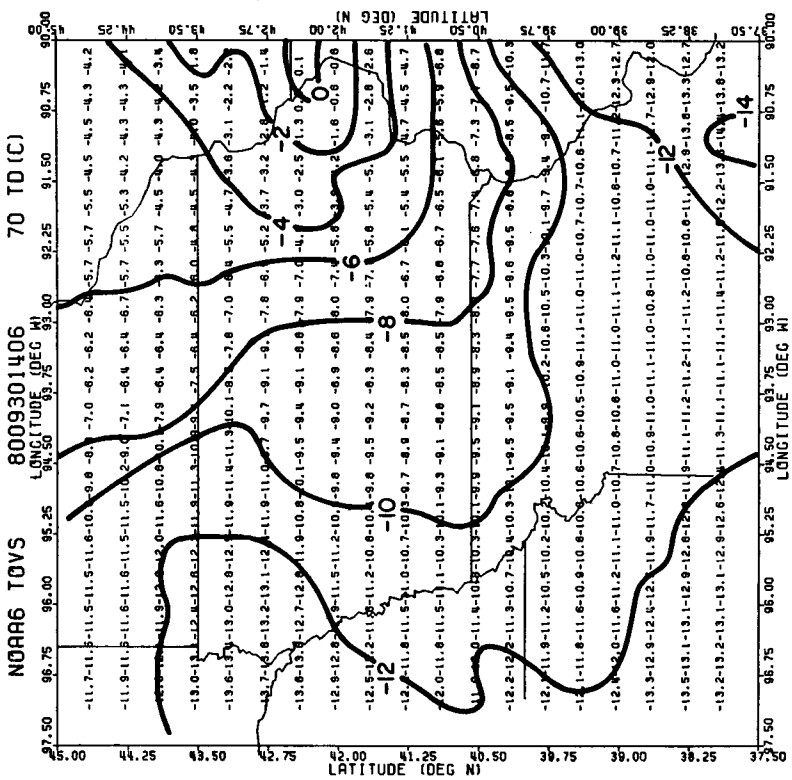

FIG. 6b. The objectively analyzed field of the data in Fig. 6a with contours every 2°C.

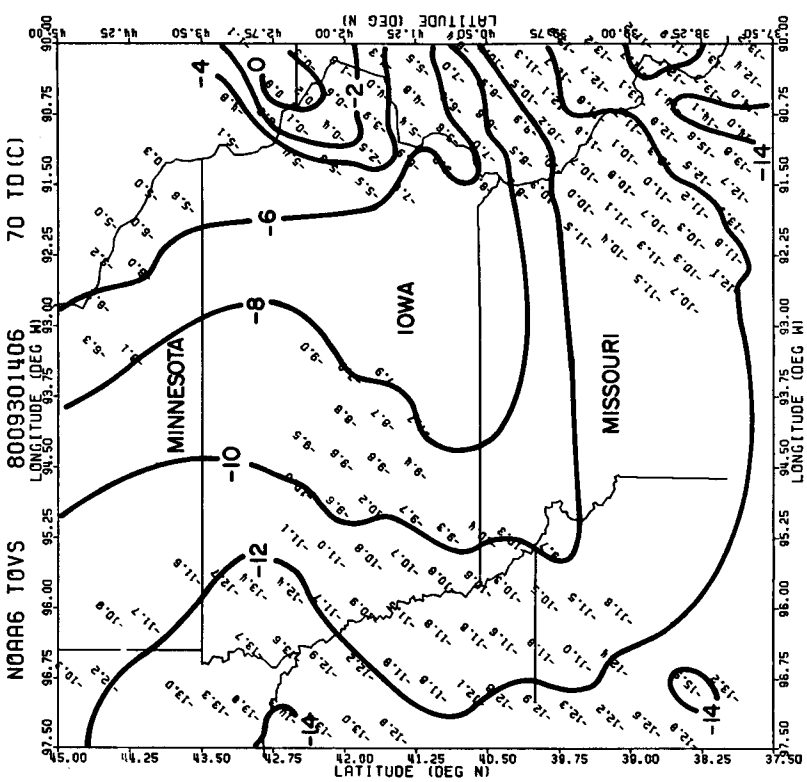

FIG. 6a. Data field of retrieved values of dew point temperature (°C) at the 70 kPa level at 1400 GMT 30 September 1980. Many data points were eliminated during retrieval due to cloud contamination. Hand drawn contours are every 2°C.

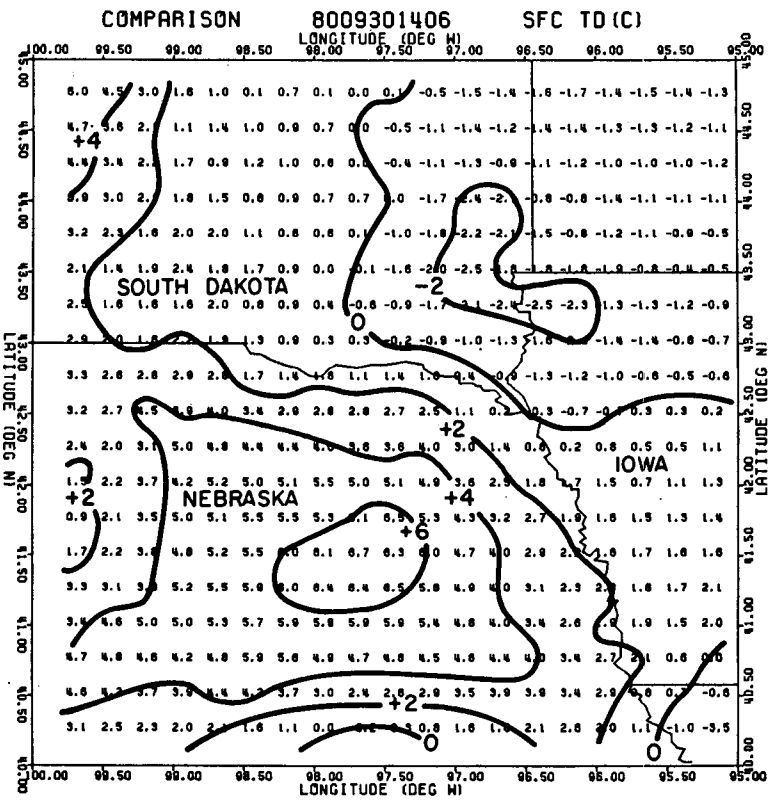

FIG. 7. A plot of the difference (°C) between surface dew point temperatures retrieved from satellite data and those measured at the surface (see text for full explanation). Averaging this field showed that the retrievals are biased by +1.75°C with respect to the surface observations. The root-mean-square difference is 2.94°C. Contours are every 2°C.

jectively analyzed using the Barnes (1964) method. Dew points were also retrieved from satellite measurements taken at 1400 GMT and were then analyzed with the technique described in this paper. The plotted values are the differences between the satellite-measured values and temporally-interpolated surface observations at 1400 GMT. A point-to-point comparison plot of this kind can be easily prepared from analyzed data, making it useful in evaluating a retrieval scheme.

4. Concluding remarks

The objective analysis method described above includes several new features which can make it a powerful tool for users of satellite data of greatly varying density. The procedure creates a complete field of parameter values at the mesh points of a regular grid, thus offering several advantages over the original nonuniformly spaced data field: 1) it allows for quick, automated *contouring* of a data field through use of existing contouring programs; 2) it provides an objective method for *comparison* of satellite-derived parameters with conventional observations on a point-to-point basis; and 3) it facilitates the *incorporation* of satellite-derived information into numerical forecast models.

One aspect of the oval-extension automated analysis that may be disadvantageous is the complexity of the procedure, which demands significant amounts of computer time to analyze even a small area. The case illustrated in Fig. 6b took 431 s of CPU time to execute on a Cyber 171 computer. The computing time is largely an increasing function of the size of the gap in the field to be analyzed.

It should also be pointed out that in this scheme the statistical information on which the weighting is based can be derived from *any* specified area of the given data set. Considering that this information is then used for interpolation into areas *without* data, the quality of the interpolation could be reduced if the statistical structure of the gap area is not largely similar to that of the specified statistical analysis area. It might, therefore, be ideal if the statistics were computed using only a small amount of data from each side of the gap. However, it is also true that a large number of points must be included in the statistical computations in order to obtain an accurate representation of the true correlations. These considerations suggest that in filling a data gap of a given size

there exists some optimum size of data-dense field from which to derive the correlation function used in filling the gap. The study reported here did not include an investigation of what that optimum size might be.

Because of the difficulty and expense of obtaining data sets for use in research and daily forecasting it is essential that all possible information be extracted from every given data source. An objective analysis procedure of the kind reported in this note is helpful in achieving that aim.

Acknowledgments. This research was supported by the Air Force Geophysics Laboratory through AFGL Contract F19628-80-C-0140. Computer time and plotting resources of the Colorado State University Computer Center were extensively utilized. The authors are indebted to Drs. Thomas Vonder Haar and Stephen Cox for their guidance and critical comments, and to Dr. C. M. Hayden of NOAA, NESS for supplying the TOVS data. We also thank Ms. Judy Sorbie for drafting many figures and Ms. Andrea Adams for typing the manuscript.

REFERENCES

Barnes, S. L., 1964: A technique for maximizing details in numerical weather map analysis. *J. Appl. Meteor.*, **3**, 396–409.

Dozier, J., 1980: Satellite identification of surface radiant temperature fields of subpixel resolution. NOAA Tech. Memo. NESS 113, 11 pp. [NTIS PB81-184038].

Gandin, L. S., 1963: *Objective Analysis of Meteorological Fields.* Gidrometeor. Izdatel., Leningrad. Israel Program for Scientific Translations, Jerusalem, 1965, 242 pp. [NTIS TT65-50007].

Ghil, M., M. Halem and R. Atlas, 1979: Time-continuous assimilation of remote-sounding data and its effect on weather forecasting. *Mon. Wea. Rev.*, **107**, 140–171.

Hillger, D. W., and T. H. Vonder Haar, 1979: An analysis of satellite infrared soundings at the mesoscale using statistical structure and correlation functions. *J. Atmos. Sci.*, **36**, 287–305.

——, and ——, 1981: Retrieval and use of high-resolution moisture and stability fields from Nimbus-6 HIRS radiances in pre-convective situations. *Mon. Wea. Rev.*, **109**, 1788–1806.

Thiebaux, H. J., 1975: Experiments with correlation representations for objective analysis. *Mon. Wea. Rev.*, **103**, 617–627.